PPAR-γ activation enhances myelination and neurological recovery in premature rabbits with intraventricular hemorrhage

Sunil Krishna[a,b,1], Bokun Cheng[a,b,1], Deep R. Sharma[a,b], Sunita Yadav[a], Erin S. Stempinski[c], Sahil Mamtani[a], Elisa Shah[a], Anjali Deo[a], Trishna Acherjee[a], Teena Thomas[a], Xusheng Zhang[d], Jinghang Zhang[e], Dumitru A. Iacobas[b,f], and Praveen Ballabh[a,b,2]

[a]Department of Pediatrics, Albert Einstein College of Medicine, Bronx, NY 10461; [b]Dominick P. Purpura Department of Neuroscience, Albert Einstein College of Medicine, Bronx, NY 10461; [c]Multiscale Microscopy Core, Oregon Health Science University, Portland, OR 97239; [d]Computational Genomics Core, Albert Einstein College of Medicine, Bronx, NY 10461; [e]Flow Cytometry Core, Albert Einstein College of Medicine, Bronx, NY 10461; and [f]Personalized Genomics Laboratory, Prairie View A&M University, Prairie View, TX 77446

Edited by Lawrence Steinman, Stanford University School of Medicine, Stanford, CA, and approved June 15, 2021 (received for review February 15, 2021)

Intraventricular hemorrhage (IVH) results in periventricular inflammation, hypomyelination of the white matter, and hydrocephalus in premature infants. No effective therapy exists to prevent these disorders. Peroxisome proliferator activated receptor-γ (PPAR-γ) agonists reduce inflammation, alleviate free radical generation, and enhance microglial phagocytosis, promoting clearance of debris and red blood cells. We hypothesized that activation of PPAR-γ would enhance myelination, reduce hydrocephalus, and promote neurological recovery in newborns with IVH. These hypotheses were tested in a preterm rabbit model of IVH; autopsy brain samples from premature infants with and without IVH were analyzed. We found that IVH augmented PPAR-γ expression in microglia of both preterm human infants and rabbit kits. The treatment with PPAR-γ agonist or PPAR-γ overexpression by adenovirus delivery further elevated PPAR-γ levels in microglia, reduced proinflammatory cytokines, increased microglial phagocytosis, and improved oligodendrocyte progenitor cell (OPC) maturation in kits with IVH. Transcriptomic analyses of OPCs identified previously unrecognized PPAR-γ–induced genes for purinergic signaling, cyclic adenosine monophosphate generation, and antioxidant production, which would reprogram these progenitors toward promoting myelination. RNA-sequencing analyses of microglia revealed PPAR-γ–triggered down-regulation of several proinflammatory genes and transcripts having roles in Parkinson's disease and amyotrophic lateral sclerosis, contributing to neurological recovery in kits with IVH. Accordingly, PPAR-γ activation enhanced myelination and neurological function in kits with IVH. This also enhanced microglial phagocytosis of red blood cells but did not reduce hydrocephalus. Treatment with PPAR-γ agonist might enhance myelination and neurological recovery in premature infants with IVH.

PPAR-γ | oligodendrocyte | microglia | myelin

Germinal matrix hemorrhage–intraventricular hemorrhage (IVH) is a major complication of prematurity, occurring in about 12,000 infants each year in the United States (1, 2). IVH leads to an accumulation of blood in the cerebral ventricle, which clogs cerebrospinal fluid (CSF) circulation and triggers an inflammatory reaction in the periventricular germinal matrix and the adjacent white matter (3). The oligodendrocyte progenitor cells (OPCs) in the periventricular germinal matrix and white matter undergo apoptotic cell death and maturational arrest, resulting in myelination failure of the white matter. CSF production is increased, and drainage is obstructed. The survivors suffer from cerebral palsy, cognitive deficits, and hydrocephalus (4–7). No effective therapeutic strategy exists against these complications of IVH. Previous studies have shown that peroxisome proliferator activated receptor-γ (PPAR-γ) agonists reduce brain inflammation and thus can be employed for the treatment of inflammatory disorders of the brain (6, 8). Indeed, the PPAR-γ agonists ameliorate neurological deficits in animal models of demyelinating disease, traumatic brain disease, and stroke (9, 10). PPAR-γ also transcriptionally up-regulates the expression of CD36 (class II scavenger receptor) on the microglial membrane, which enhances microglial phagocytosis and hematoma clearance (11). However, the effects of PPAR-γ activation on OPC maturation, myelination, and microglial activation have not been studied in the developing brain during the perinatal period. Therefore, we asked whether PPAR-γ up-regulation improved myelination, prevented hydrocephalus, and enhanceed neurological recovery in preterm newborns with IVH.

PPAR-γ belongs to the nuclear receptor superfamily and is expressed in neurons, microglia, macrophages, astrocytes, and oligodendrocytes (12–14). It regulates the expression of genes controlling lipid and carbohydrate metabolism and thus influences lipid metabolism and insulin sensitivity (15, 16). The brain is enriched in lipids, and oligodendrocytes are the major lipid synthesizing cells (15). PPAR-γ drives the expression of enzymes, including lipoprotein lipase and fatty acid transport proteins, which are involved in lipid uptake and play key roles in OPC differentiation programs (17). Consistent with this notion, a few studies show that

Significance

Intraventricular hemorrhage (IVH) is the most common neurological disorder of premature infants and remains a major cause of white matter injury in the survivors. No therapeutic strategy exists to prevent IVH-induced hypomyelination and cerebral palsy in these infants. We showed that pharmacological or genetic activation of peroxisome proliferator activated receptor-γ (PPAR-γ) ameliorated inflammation, oligodendrocyte progenitor cell (OPC) maturation, myelination, and motor function in rabbit kits with IVH. PPAR-γ activation also promoted microglial phagocytosis but did not reduce hydrocephalus. Transcriptomic analyses identified previously unrecognized PPAR-γ–induced genes in the isolated OPCs and microglia, which would reprogram these cells toward reducing inflammation and promoting myelination. The study highlights PPAR-γ–induced reversal of white matter injury in premature newborns with IVH and the underlying mechanisms.

Author contributions: P.B. designed research; S.K., B.C., D.R.S., S.Y., E.S.S., S.M., E.S., A.D., T.A., T.T., X.Z., J.Z., and P.B. performed research; S.K., B.C., D.A.I., and P.B. analyzed data; and D.A.I. and P.B. wrote the paper.

The authors declare no competing interest.

This article is a PNAS Direct Submission.

[1]S.K. and B.C. contributed equally to this work.

[2]To whom correspondence may be addressed. Email: praveen.ballabh@einsteinmed.org.

This article contains supporting information online at https://www.pnas.org/lookup/suppl/doi:10.1073/pnas.2103084118/-/DCSupplemental.

Published August 30, 2021.

PPAR-γ enhances survival and maturation of OPCs in a culture model (18). Moreover, PPAR-γ activation reduces inflammation and oxidative stress in adult models of intracranial hemorrhage by down-regulating proinflammatory cytokines, matrix metalloproteinase-9 (MMP9), inducible nitric oxide synthase expression, and extracellular H_2O_2 level as well as up-regulating catalase and CD36 (11). Thus, PPAR-γ activation might reduce IVH-induced inflammation and free radical generation, enhancing survival and maturation of OPCs as well as neurological recovery (19).

PPAR-γ is a ligand-dependent transcription factor that is activated by both synthetic and naturally occurring compounds including Thiazolidinediones, 15-deoxy prostaglandin-J1, and long chain fatty acids. PPAR-γ agonists, rosiglitazone and pioglitazone, have shown promise as a therapeutic agent in animal models of a wide range of neurological disorders including demyelinating and neurodegenerative diseases, traumatic injuries, and stroke (20, 21). In addition, both rosiglitazone and pioglitazone attenuate infarct volume and are neuroprotective in an adult mouse model of ischemia (10, 22). Rosiglitazone is currently in clinical use in diabetic patients for reducing blood glucose. However, the Food and Drug Administration has proposed a warning that rosiglitazone (Avandia) treatment increases ischemic cardiovascular risk. Since ischemic heart disease is predominantly a problem of adults, rosiglitazone treatment is expected to be safe in newborns.

Although PPAR-γ agonists offer neuroprotection by reducing inflammation, alleviating free radical generation, and enhancing clearance of debris and red blood cells (9, 23), the effect of PPAR-γ activation in reprogramming OPC and microglial transcriptomics, OPC maturation, and myelination has not been studied specifically in a preterm-born animal model of IVH. We hypothesized that both genetic and pharmacological up-regulation of PPAR-γ would enhance OPC maturation, myelination, and neurological recovery in rabbits with IVH. We also postulated that PPAR-γ stimulation might reduce posthemorrhagic hydrocephalus via activation of CD36 receptors. We tested these hypotheses in rabbit kits with IVH and found that rosiglitazone or Ad-PPAR-γ treatment enhanced myelination and neurological recovery in rabbit kits with IVH but did not reduce hydrocephalus. RNA sequencing (RNA-seq) of isolated OPC and microglia identified important PPAR-γ–induced genes that likely contributed to the neurological recovery.

Results

IVH Induces PPAR-γ Expression in the Microglia of Human Preterm Infants. To determine how the expression of PPAR-γ changes with the occurrence of IVH, we evaluated the immunoreactivity of PPAR-γ in microglia, OPCs, and astrocytes in postmortem samples from premature human infants with and without IVH. To this end, we immunostained coronal sections from the frontoparietal cortex of preterm infants of 23 to 28 wk of gestational age. Triple labeling with PPAR-γ–, Iba1-, and glial fibrillary acidic protein (GFAP)-specific antibodies revealed that PPAR-γ was abundantly expressed by $Iba1^+$ microglia/macrophages in the periventricular white matter and ganglionic eminences of infants with IVH but scarcely in infants without IVH (Fig. 1). Accordingly, quantification showed that both total $Iba1^+$ and $Iba1^+PPAR\text{-}\gamma^+$ cells were significantly greater in density in infants with IVH compared with controls without IVH ($P < 0.001$ for both). Moreover, PPAR-γ expression was weak to absent on GFAP astrocytes in the periventricular white matter and ganglionic eminence of both infants with and without IVH.

Double labeling of coronal sections with PPAR-γ–, O4-, and Olig2-specific antibodies showed that PPAR-γ was expressed by a few $O4^+$ OPCs in the developing white matter and ganglionic eminences of both infants with and without IVH (Fig. 1). Similarly, PPAR-γ was expressed infrequently by $Olig2^+$ OPCs in preterm infants with and without IVH. Together, IVH induces PPAR-γ expression in microglia, which is scarcely and weakly expressed on OPCs and astrocytes.

IVH Increases PPAR-γ Expression in Microglia in Preterm Rabbits but Not on OPCs. Since IVH increased the PPAR-γ expression in microglia/macrophages of preterm human infants, we next evaluated the effect of IVH on PPAR-γ expression on neural cells in preterm rabbits. Thus, we doubled labeled coronal brain sections from E29 rabbit kits with Iba1- and PPAR-γ–specific antibodies and found that the number of total $Iba1^+$ and $PPAR\text{-}\gamma^+Iba1^+$ microglia was higher in the periventricular white matter and ganglionic eminence of preterm kits with IVH compared with glycerol-treated controls without IVH at postnatal day (D) 3 ($P < 0.01$, Fig. 2 *A* and *B*). However, PPAR-γ expression was weak to absent on $O4^+$ and $Olig2^+$ OPCs as well as on $GFAP^+$ astrocytes in kits with and without IVH at both D3 and D7. We next performed Western blot analyses to quantify PPAR-γ expression in the coronal slice (midseptal nucleus level) of the forebrain from kits with and without IVH. PPAR-γ expression was comparable between kits with IVH and controls without IVH (glycerol-treated and untreated) at both D3 and D7 (Fig. 2*C*). However, RT-qPCR revealed that PPAR-γ messenger RNA (mRNA) expression was higher in rabbits with IVH compared with controls without IVH at D3 ($P = 0.0482$) but not at D7 (Fig. 2*D*). The failure to detect elevated levels of PPAR-γ in kits with IVH in Western blot analyses could be due to high protein turnover or to a relatively small and imperceptible increase in PPAR-γ protein levels in kits with IVH. Together, IVH increases PPAR-γ transcription and elevates PPAR-γ protein levels in $Iba1^+$ microglia/macrophages of the periventricular germinal matrix and white matter.

PPAR-γ Activation or Overexpression Increases Microglial Density in Kits with IVH. Since activation of PPAR-γ enhances neurological outcome in a number of animal models of brain injury (10, 11), we reasoned that increasing PPAR-γ expression might enhance molecular, histological, and clinical outcome of rabbit kits with IVH. To activate PPAR-γ signaling, we employed two strategies: 1) rosiglitazone treatment, a PPAR-γ agonist, and 2) PPAR-γ (cytomegalo virus [CMV] promoter) adenoviral delivery. To this end, we randomized rabbit kits with IVH into two groups—rosiglitazone and vehicle treatment. We quantified the number of microglia coexpressing Iba1 and PPAR-γ. We found that the density of $Iba1^+PPAR\text{-}\gamma^+$ microglia was threefold higher in rosiglitazone-treated kits with IVH relative to vehicle controls with IVH ($P < 0.001$, *SI Appendix*, Fig. S1 *A* and *B*). In addition, the density of total $Iba1^+$ microglia was also elevated in rosiglitazone-treated kits with IVH relative to vehicle controls ($P < 0.001$). Consistent with rosiglitazone treatment, Ad-PPAR-γ administration increased the density of $Iba1^+PPAR\text{-}\gamma^+$ microglia compared with Ad-GFP controls ($P = <0.001$, *SI Appendix*, Fig. S1*C*). However, the density of all $Iba1^+$ microglia was similar between the two groups. Together, rosiglitazone treatment or adenoviral delivery of the PPAR-γ gene increases the total number of $Iba1^+PPAR\text{-}\gamma^+$ microglia.

We next evaluated coronal sections double-labeled with O4- and PPAR-γ–specific antibodies. We found that the number of $O4^+$ OPCs expressing PPAR-γ were elevated in the periventricular corona radiata of Ad-PPAR-γ–treated kits with IVH compared with Ad-GFP–treated controls at D7 ($P < 0.001$, *SI Appendix*, Fig. S2). About 18% of all $O4^+$ OPCs expressed PPAR-γ in Ad-PPAR-γ–treated kits, whereas PPAR-γ–expressing $O4^+$ cells were almost absent in Ad-GFP–treated kits. Ad-PPAR-γ treatment did not affect the total number of $O4^+$ OPCs. Together, PPAR-γ overexpression by Ad-PPAR-γ treatment increased microglial density and enhanced the expression of PPAR-γ on OPCs.

Rosiglitazone or Ad-PPAR-γ Treatment Enhances Myelination. Since PPAR-γ agonists protect oligodendrocytes and prevent demyelination in animal models of multiple sclerosis (24), we postulated that pharmacological activation by PPAR-γ agonist or genetic overexpression of PPAR-γ might promote myelination in rabbit kits with IVH. We thus compared myelination between three groups

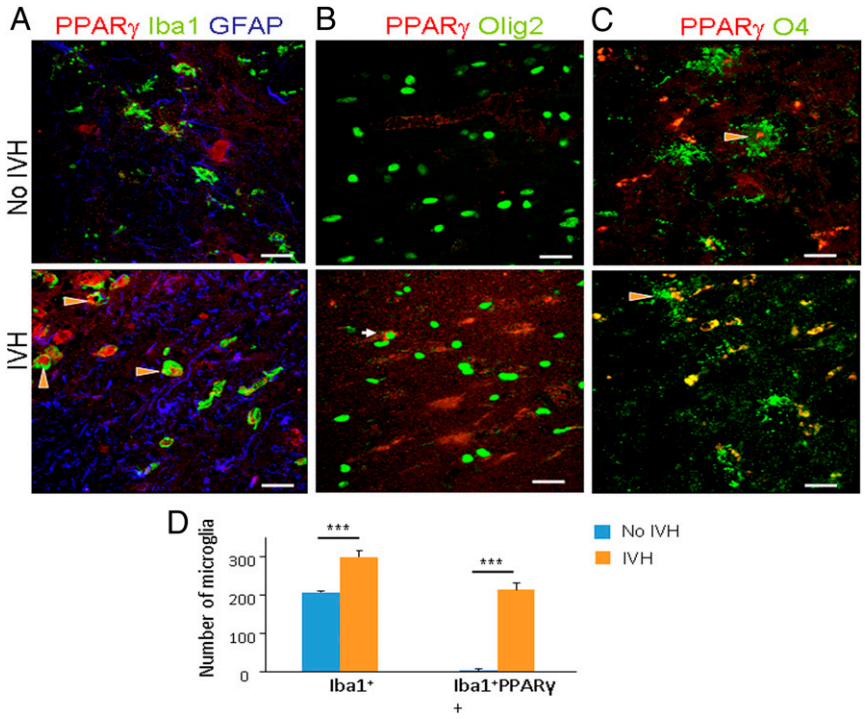

Fig. 1. IVH triggers PPAR-γ expression on microglia in human preterm infants. (*A–C*) Representative immunofluorescence of cryosections from infants with and without IVH of 23 wk gestation, which were labeled using (*A*) PPAR-γ, Iba1, and GFAP, (*B*) PPAR and Olig2, and (*C*) PPAR- and O4-specific antibodies. PPAR-γ $^{+}$Iba1^{+} cells (arrowhead) are abundant in infants with IVH but infrequent in newborns without IVH. GFAP^{+} radial glia in the ganglionic eminence and astrocytes in the embryonic whiter matter did not express PPAR-γ. PPAR-γ was expressed only on a few O4^{+} (arrowhead) or Olig2^{+} (arrow) OPCs. (Scale bar, 20 μm.) (*D*) Bar charts are mean ± SEM ($n = 5$ each). Quantification showed that both the total Iba1^{+} and Iba1^{+} PPAR-γ^{+} cells were significantly higher in number in infants with IVH compared with controls without IVH (two-way ANOVA). ***$P < 0.001$. (Scale bar, 20 μm.)

of rabbit kits at D14: 1) kits without IVH (glycerol-treated), 2) kits with IVH (vehicle-treated), and 3) rosiglitazone-treated kits with IVH. We used intraperitoneal (IP) glycerol to induce IVH in E29 kits (term E32) at 3 to 4 h of age (Fig. 3*A*), and then the kits with IVH were treated with either intramuscular (IM) rosiglitazone or vehicle to evaluate the effect of the PPAR-γ agonist on myelin formation. We measured the severity of IVH by head ultrasound, which was comparable between groups. We quantified myelin basic protein (MBP) in the immunolabeled sections stereologically and found that the volume fractions of MBP in the periventricular white matter were reduced in kits with IVH relative to controls without IVH ($P < 0.049$, Fig. 3*B*). More importantly, the volume fraction of MBP was elevated in rosiglitazone-treated kits relative to vehicle controls ($P = 0.038$). In agreement with the stereological quantification, Western blot analyses showed that MBP and myelin-associated glycoprotein (MAG) levels were reduced in kits with IVH compared with glycerol controls without IVH ($P < 0.001$, both) and that rosiglitazone treatment significantly raised levels of MBP and MAG in kits with IVH ($P = 0.047$ and 0.03, respectively; Fig. 3*C*).

Rosiglitazone is a pharmacological compound and can exhibit nonspecific effects. Thus, to selectively and specifically up-regulate PPAR-γ, we injected Ad-PPAR-γ adenovirus into the lateral ventricles and compared the extent of myelin in the white matter between Ad-PPAR-γ and Ad-GFP–treated kits. Consistent with the rosiglitazone treatment, the volume fraction of MBP in the corona radiata and corpus callosum was higher in Ad-PPAR-γ–treated animals compared with Ad-GFP controls ($P = 0.02$, Fig. 4*A*). Moreover, Western blot analyses demonstrated higher MBP and MAG expression in Ad-PPAR-γ–treated kits compared with Ad-GFP controls ($P < 0.003$ and 0.001, Fig. 4*B*), respectively.

Ultrastructural evaluation of the corpus callosum and corona radiata in the white matter showed that Ad-PPAR-γ treatment expanded the mean density of myelinated axons to ∼170% in kits with IVH. However, the comparison was not statistically significant (Fig. 4*C*). In addition, the g-ratio was similar between Ad-PPAR-γ or Ad-GFP–treated kits, consistent with our previous studies of improved myelination through thyroxine treatment (25). Together, rosiglitazone or Ad-PPAR-γ treatment enhances myelination in kits with IVH, which confirms a definite role of Ad-PPAR-γ in promoting myelination in developing brains with IVH.

Rosiglitazone Treatment Enhances Neurological Recovery. The premature infants with IVH often develop motor deficits (7). We, therefore, evaluated the effect of IVH and the impact of PPAR-γ activation in kits with IVH by performing open field tests at D14, using Any-Maze software. We compared three groups of kits, including kits without IVH, kits with IVH treated with rosiglitazone, and kits with IVH exposed to vehicle. We found that kits with IVH were less active and traveled a shorter distance in the arena compared with kits without IVH ($P = 0.03$ both, one-way ANOVA, Tukey's post hoc test, Fig. 5 *A* and *B*). In addition, kits with IVH had slower speed in the entire arena and in the center of the arena relative to kits without IVH ($P = 0.02$, 0.008, one-way ANOVA, Tukey's post hoc test). Kits treated with rosiglitazone were significantly more active for a longer time compared with vehicle controls ($P = 0.048$). The distance traveled and speed within both the entire and central arena showed a trend toward increase in rosiglitazone-treated kits compared with vehicle controls; however, the comparison was not statistically significant (Fig. 5 *C* and *D*). Together, treatment with PPAR-γ agonist improves the motor function of kits with IVH.

Rosiglitazone or Ad-PPAR-γ Reduces Inflammation and Astrogliosis. Since the inhibition of inflammation promotes myelination (19), we reasoned that the improvement in myelination could be a

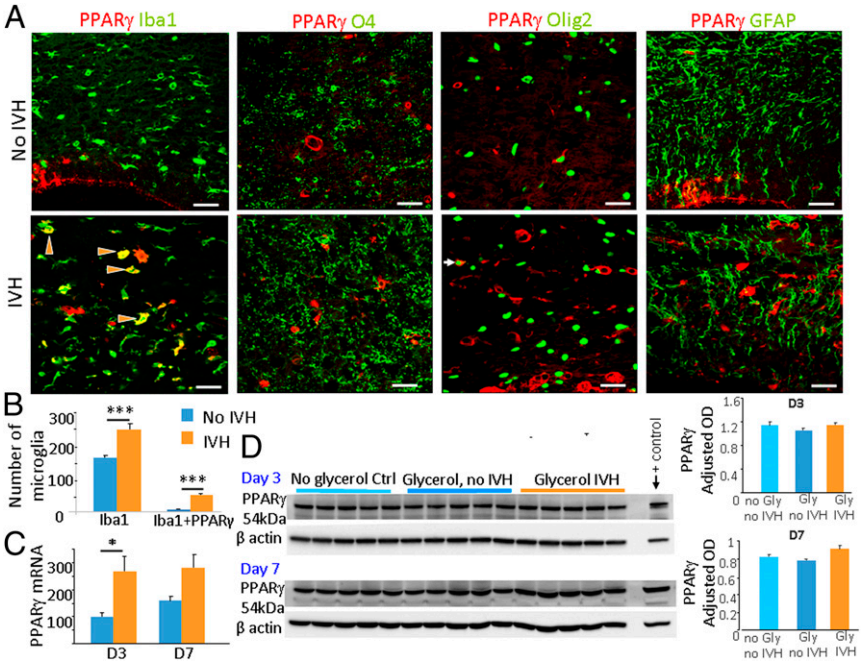

Fig. 2. IVH induces PPAR-γ expression on microglia of preterm rabbit kits. (*A*) Representative immunofluorescence from the medial ganglionic eminence of 3-d-old prematurely delivered (E29) rabbit kits with and without IVH. Coronal sections were double-labeled using PPAR-γ with O4, Olig2, Iba1, or GFAP-specific antibodies (as indicated). Note that PPAR-γ was expressed in Iba1$^+$ microglia in kits with IVH (arrowhead), but its expression was almost absent in kits without IVH. PPAR-γ reactivity was weak to absent on O4$^+$ OPCs, Olig2$^+$ OPCs (arrow), and GFAP$^+$ astrocytes. (*B*) Bar graphs show the mean ± SEM ($n = 5$ each group). Iba1$^+$ and PPAR-γ$^+$Iba1$^+$ microglia were higher in numbers in kits with IVH compared with controls without IVH at D3. (*C*) mRNA expression of PPAR-γ was higher in kits with IVH relative to the controls without IVH at D3 but not at D7. (*D*) A typical Western blot showing PPAR-γ levels in three groups of kits, as indicated, at 3 and 7 d. Bar graphs show the mean ± SEM ($n = 5$ each group). PPAR-γ protein concentration was normalized to β-actin. Note that PPAR-γ levels were comparable between kits with IVH, glycerol-treated controls, and untreated controls without IVH at both D3 and D7. *$P < 0.05$ and ***$P < 0.001$. (Scale bar, 20 μm.)

result of PPAR-γ–induced reduction in inflammation (19). Thus, we postulated that rosiglitazone or Ad-PPAR-γ treatment reduced inflammation and astrogliosis. To this end, we quantified mRNA expression of proinflammatory cytokines by RT-qPCR using TaqMan probes and compared them between kits with and without IVH. We found that the mRNA expression of TNF-α, IL6, and LIF were higher in kits with IVH compared with controls at D3 ($P = 0.013$, 0.014, and 0.049, *SI Appendix*, Fig. S3*A*) but not at D7. IL1-β levels were similar between kits with and without IVH at both D3 and D7. We next evaluated the effect of rosiglitazone or Ad-PPAR-γ treatment on these cytokines in kits with IVH relative to their vehicle controls. We found that rosiglitazone treatment diminished the levels of TNF-α and LIF at D3 ($P = 0.03$, 0.003; *SI Appendix*, Fig. S3*B*) but not at D7. Rosiglitazone did not affect IL-6 or IL1-β mRNA expression. The Ad-PPAR-γ treatment reduced mRNA accumulation of IL-6 and LIF at D7 (0.007, 0.047 respectively, *SI Appendix*, Fig. S3*C*) but not TNF-α and IL1-β expressions. The data suggest that rosiglitazone or Ad-PPAR-γ treatment down-regulates some of the proinflammatory cytokines and thereby inhibits inflammation.

We next quantified astrogliosis in GFAP immunostained sections following a stereology protocol. Our analysis demonstrated that the total volume fraction (load) of astrocyte cell bodies and their fibers was significantly increased in kits with IVH compared with controls without IVH ($P < 0.001$). More importantly, rosiglitazone treatment reduced the volume fraction of GFAP$^+$ astrocyte arborizations in the corpus callosum relative to vehicle controls with IVH ($P = 0.004$, *SI Appendix*, Fig. S4*A*). Western blot analyses revealed that GFAP levels showed a trend toward decline but were not significantly reduced in rosiglitazone-treated kits compared with vehicle controls (*SI Appendix*, Fig. S4*B*). Just like rosiglitazone treatment, Ad-PPAR-γ administration significantly reduced the volume fraction of GFAP$^+$ astrocytes compared with Ad-GFP controls ($P < 0.001$, *SI Appendix*, Fig. S4*C*). However, GFAP protein, measured by Western blot analyses, was comparable between the two comparison groups. Together, rosiglitazone or Ad-PPAR-γ treatment reduces inflammation and astrocytic arborization in the periventricular white matter of kits with IVH.

Rosiglitazone Treatment Promotes the Maturation of OPCs. Our previous studies have shown that the occurrence of IVH reduces proliferation of platelet-derived growth factor receptor (PDGFR)-α$^+$ preoligodendrocytes and inhibits maturation of OPCs (26). Since PPAR-γ activation by rosiglitazone treatment enhanced myelination in the present study, we postulated that PPAR-γ activation enhances proliferation and maturation of OPCs. To this end, we double-labeled coronal sections with PDGFR-α and Ki67-specific antibodies to assess proliferation of early OPCs in the corona radiata and corpus callosum. We found that rosiglitazone treatment did not affect the density of total or cycling PDGFR-α$^+$ progenitors at D3 (*SI Appendix*, Fig. S5*A*).

We next assessed the maturation of OPCs by double labeling the coronal sections with Nkx2.2- and Olig2-specific antibodies. Nkx2.2$^+$ cells label myelinating (immature) OPCs, and Olig2 stains most of the OPCs and mature oligodendrocytes. We found that the rosiglitazone treatment increased the density of Olig2$^+$Nkx2.2$^+$ OPCs ($P = 0.003$) but did not affect the population of total Olig2$^+$ cells (*SI Appendix*, Fig. S5*B*). This suggests that rosiglitazone treatment promotes the maturation of OPCs in kits with IVH. Consistent with this finding, we found that the levels of CNPase (2,3-cyclic nucleotide-3-phosphodiesterase), measured by Western blot analyses, were significantly reduced in kits with IVH compared with controls without IVH ($P = 0.01$) and were elevated on rosiglitazone treatment ($P = 0.03$, one-way ANOVA, *SI Appendix*,

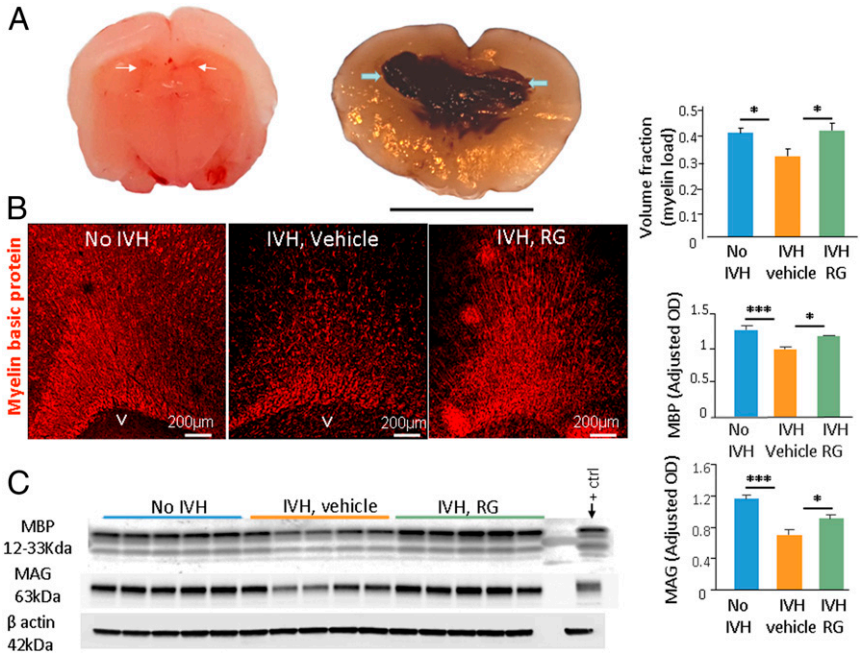

Fig. 3. Rosiglitazone treatment enhances myelination. (*A*) Coronal section through the frontal lobe of E29 rabbit pups showing slit-like ventricles without any hemorrhage (arrows, *Left*) and severe hemorrhage resulting in the fusion of the two ventricles (arrowheads, *Right*). (Scale bar, 1 cm.) (*B*) Representative immunofluorescence of MBP in the corona radiata of 14-d-old kits. Bar chart indicates mean ± SEM ($n = 5$ in each group). The volume fraction of MBP was elevated in the rosiglitazone (RG)-treated kits compared with vehicle controls. (*C*) Representative Western blot analysis for MBP in the forebrain of three sets of premature rabbit kits, as indicated at 14 d. Each lane represents lysate made from a whole coronal slice taken at the level of the midseptal nucleus of the brain. MBP concentration was normalized to β-actin. The bar graph shows the mean ± SEM ($n = 5$ in each group). MBP and MAG expression was higher in rosiglitazone-treated kits compared with vehicle controls at D14. (Scale bar, 200 μm.) v, ventricle. $^*P < 0.05$ and $^{***}P < 0.001$ for the comparison between groups as depicted.

Fig. S5*C*). Together, rosiglitazone treatment promotes myelination by enhancing maturation of OPCs and does not impact their proliferation.

PPAR-γ Activation Increases the Number of CD36$^+$ Microglia and Phagocytosis but Does Not Reduce Hydrocephalus. Since PPAR-γ activation up-regulates CD36 expression on microglial membrane, enhances microglial phagocytosis, and promotes hematoma clearance in an adult model of intracranial hemorrhage (ICH) (11), we hypothesized that PPAR-γ activation would up-regulate CD36 expression, enhance phagocytosis of red blood cells, and reduce hydrocephalus in preterm kits with IVH. To this end, we measured CD36 expression in kits with and without IVH as well as in kits with IVH who were treated with either Ad-PPAR-γ or rosiglitazone. RT-qPCR using the TaqMan probe revealed that CD36 mRNA accumulation showed a trend toward elevation in kits with IVH compared with controls without IVH at both D3 and D7, but the comparison was statistically insignificant (Fig. 6*A*). We next assessed the effect of rosiglitazone and Ad-PPAR-γ treatment. We found that rosiglitazone or Ad-PPAR-γ treatment resulted in a trend toward elevation of CD36 mRNA levels compared with their respective controls, but the comparisons were not statistically significant.

We next evaluated the effect of Ad-PPAR-γ treatment on CD36$^+$ microglia in immunolabeled coronal brain sections compared with Ad-GFP controls. We found that the density of Iba1$^+$CD36$^+$ microglia were higher in Ad-PPAR-γ–treated kits with IVH compared with Ad-GFP controls with IVH at D7 ($P = 0.001$, Fig. 6*B*). This suggests that PPAR-γ activation expands the number of CD36$^+$ microglia.

Since CD36 is a phagocytic receptor and is elevated on the microglial cell membrane, we reasoned that this might activate microglial phagocytosis. To this end, we assigned animals with IVH into four groups: IM rosiglitazone, IM vehicle, intracerebroventricular (ICV) Ad-PPAR-γ and ICV Ad-GFP treatment. We next injected 2.5 μL fluorescent latex beads (1 μ diameter, yellow-green) into the lateral ventricle at 24 h age. The kits were euthanized at 72 h after the initiation of rosiglitazone or Ad-PPAR-γ treatment, and sections were stained with Iba1 antibody. The phagocytic index (percentage of microglia$^+$ for beads × mean number of beads per microglia) was computed. We found that the phagocytic index was higher in rosiglitazone- and Ad-PPAR-γ–treated kits compared with their respective controls ($P < 0.02$, 0.045, respectively, Fig. 6*C*).

To compare the development of hydrocephalus and its severity, we compared ventricle volume measured by head ultrasound in rosiglitazone-treated kits with vehicle controls at D14. We found that ventricle volume was comparable between rosiglitazone- and vehicle-treated kits (Fig. 6*D*). Similarly, ventricle volume was similar between Ad-PPAR-γ and Ad-GFP kits at D14. Together, PPAR-γ–induced up-regulation of CD36 enhances microglial phagocytosis without minimizing the occurrence of hydrocephalus.

RNA-seq of Isolated Microglia from Ad-PPAR-γ (CMV Promoter)–Treated Animals. To address the effect of PPAR-γ overexpression on the microglial transcriptome, we performed an RNA-seq analysis on CD45^{Low}/CD11b$^+$ microglia isolated from the cerebral hemispheres of Ad-PPAR-γ or Ad-GFP–treated kits with IVH by fluorescence activated cell sorting (FACS) at D7 (*SI Appendix*, Fig. S6 *A–E*). Sequencing data were deposited in the National Center for Biotechnology Information Gene Expression Omnibus. Expressions of 11,069 genes were adequately quantified and compared between Ad-PPAR-γ– and Ad-GFP–treated kits by employing two methods: 2) expression ratio (x) and b) weighted individual (genes) regulations (WIR, Fig. 7). About 12% of genes (1,316) were significantly different between the two groups. Of these, 606 genes

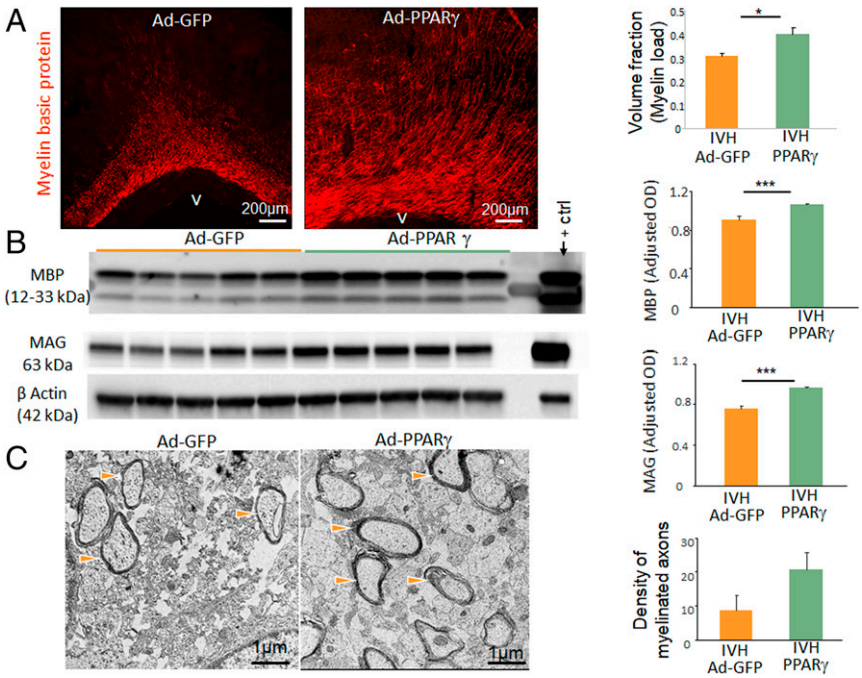

Fig. 4. Ad-PPAR-γ treatment enhances myelination. (*A*) Representative immunostaining of the coronal section with MBP antibody of 14-d-old kits. Note immunoreactivity for MBP in the periventricular corona radiata is higher in Ad- PPAR-γ–treated kits relative to Ad-GFP controls. Error bars indicate mean ± SEM ($n = 5$ in each group). The volume fraction of MBP (myelin load) was elevated in Ad-PPAR-γ–treated kits compared with Ad-GFP–treated controls. (Scale bar, 200 μm.) (*B*) Representative Western blot analysis for MBP in the forebrain of three sets of premature rabbit kits at D14, as indicated. Each lane represents lysate from a whole coronal slice taken at the level of the midseptal nucleus of a brain. The bar graph shows the mean ± SEM ($n = 5$ in each group). MBP concentration was normalized to β-actin. MBP and MAG expression was higher in Ad-PPAR-γ–treated kits compared with Ad-GFP controls. (*C*) Typical electron micrograph from rabbit kits with IVH treated with Ad-PPAR-γ and Ad-GFP. Note that myelinated axons (arrowhead) were more abundant in kits treated with Ad-PPAR-γ compared with Ad-GFP controls. $*P < 0.05$, $**P < 0.01$, and $***P < 0.001$ for the comparison between groups as depicted. V, ventricle.

were up-regulated, whereas 710 genes were down-regulated in the microglia of Ad-PPAR-γ–treated kits compared with Ad-GFP controls. Five genes, dehydrogenase/reductase 9, exostosin like glycosyltransferase 1, MICAL C-terminal like, stanniocalcin 2, and ENSOCUG00000008343, were turned off, and two genes, ENSOCUG00000016801 and ENSOCUG00000024794, were turned on. KEGG (Kyoto Encyclopedia of Genes and Genomes) pathway analyses revealed that genes for oxidative phosphorylation, glycolysis–gluconeogenesis, cytokine–cytokine receptor interaction (inflammatory), amyotrophic lateral sclerosis, and Parkinson's disease were significantly altered in the microglia of Ad-PPAR-γ–treated animals relative to Ad-GFP controls, indicating PPAR-γ–induced reprogramming of the microglial cells (Fig. 7 *A–F* and *SI Appendix*, Fig. S6*F*). Several genes for oxidative phosphorylation, including NADH (nicotinamide adenine dinucleotide hydrogen) dehydrogenase 1 (complex 1: *ND1*, *Ndufa3*, *Ndufa7*, *Ndufb2*, *Ndufb6*, *Ndufc1*, *Ndufs3*), cytochrome *b*-c1 complex subunit 7 (complex 3: subunit 6 and 7, *UQCRQ*), cytochrome b5 type B, cytochrome *c* oxidase (complex 4, subunit 5B and C, and Cox6A1), adenosine triphosphate (ATP) synthase, and V-type proton ATPase were reduced in the microglia of Ad-PPAR-γ–treated kits compared with controls (Fig. 7 *A* and *B*). In addition, genes for the enzymes of the glycolytic pathway, including *ENO1*, *ENO2*, *GAPDH*, *GPI*, *HK3*, *LDHA*, *PGAM1*, *PCK2*, *PGK1*, and *TPI1*, were significantly down-regulated in the microglia of Ad-PPAR-γ–treated kits (Fig. 7 *A* and *C*). Reduction of these genes in the two pathways would reduce ATP generation in both the mitochondria and the cytosol. Among genes mediating inflammation, interleukin1-receptor 2 (*IL1R2*, suppressor of IL-1) and interferon regulatory factor 7 (*IRF7*) were elevated, but macrophage inhibiting factor (*MIF*) was reduced in Ad-PPAR-γ–treated kits with IVH relative to controls (Fig. 7*D* and *SI Appendix*, Fig. S6*F*). These changes would contribute to a reduction in cerebral inflammation (27–29). Moreover, gene expression of kynurenine 3-monooxygenase (*KMO*), annexin-A1, -A2, -A3, -A4, -A5 (*ANXA1-5)* was reduced, and the *S100A9* level was increased in Ad-PPAR-γ–treated kits relative to controls, which would also contain IVH-induced inflammation. A significant reduction in MMP9 enzyme in PPAR-γ–overexpressed animals would reduce the tissue injury. However, cytokines (*IL1A*, *IL1B*, *IL6R*, *IL 7*, *TNF*), chemokines (*CCL2*, *CCL14*, *CCL24*, *CXCL8*), and chemokine receptors (*CCR1*, *CCR5*) were also elevated in Ad-PPAR-γ–treated kits, which might accentuate inflammation. Genes playing key roles in amyotrophic lateral sclerosis (ATP synthase, NADH dehydrogenase 1, and others) and Parkinson's disease (*PARK7*, *PLCG1*, *PSMB5*, *TUBA4A*, and ATP synthases) were also reduced (Fig. 7*E* and *SI Appendix*, Fig. S6*F*). *CCL2*, *COLEC2*, and *TAGLN2* genes, having roles in phagocytosis and host defense (30, 31), were elevated in Ad-PPAR-γ–treated kits with IVH relative to Ad-GFP controls.

Although elevation in PPAR-γ expression resulted in beneficial changes in the expression of several genes, a few genes with harmful effects were also elevated. For example, an elevation in *FBXO10* (proapoptotic), Steap-4 (increases oxidative stress), and some proinflammatory cytokines can exert detrimental effects. Together, overexpression of PPAR-γ reprograms microglial function, which likely reduces inflammation and tissue injury.

RNA-seq of Isolated OPCs from Ad-PPAR-γ (CMV promoter)–Treated Animals. To determine the effect of PPAR-γ overexpression on OPC transcriptome, we performed an RNA-seq analysis on $O4^+$ OPC isolated from the cerebral hemispheres of Ad-PPAR-γ and Ad-GFP–treated preterm kits with IVH at D7. The expressions of 11,040 genes were adequately quantified. Of these, the expression of 134 genes were significantly elevated, and 81 genes were reduced

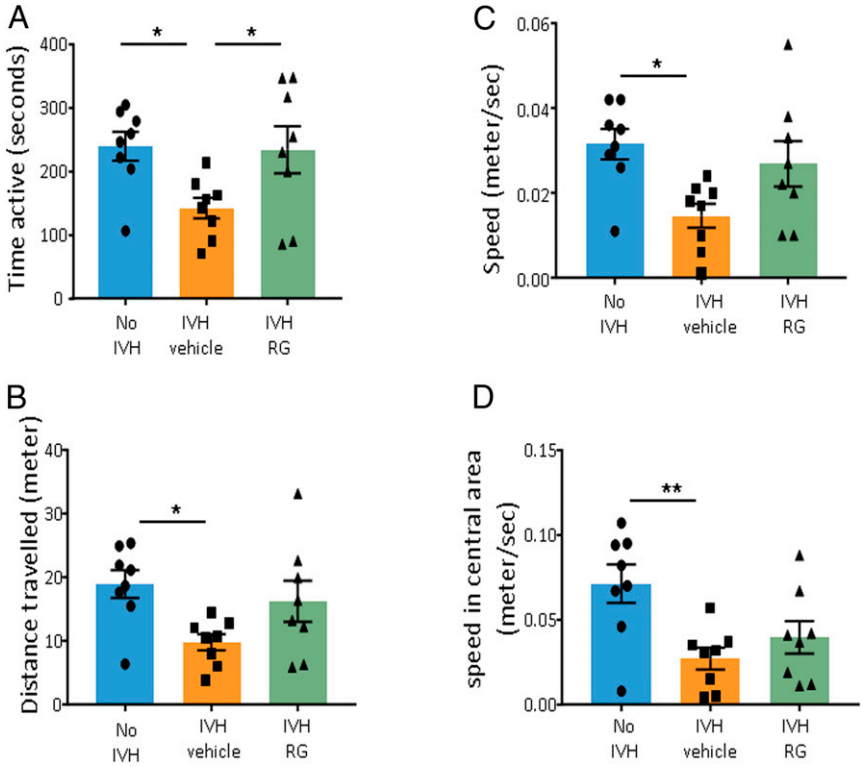

Fig. 5. Rosiglitazone (RG) treatment enhances motor function. Bart charts are mean ± SEM ($n = 8$ to 9 in each group). An open field test was performed using Any-Maze on day 14. Kits with IVH were less active, traveled less distance, and displayed less speed both in the center and whole arena compared with controls without IVH (*A–D* as indicated). Kits treated with RG were active for a significantly longer time compared with vehicle-treated control with IVH. $*P < 0.05$ and $**P < 0.01$.

in Ad-PPAR-γ–treated compared with Ad-GFP–treated kits with IVH. Our analyses showed that the gene sets for purinergic signaling, fatty acid synthesis, other metabolic pathways, cell cycle, antioxidants, and PPAR-γ were altered, which can affect oligodendrogenesis (Fig. 8 *A* and *B*) (32–34). *P2X4* is a purinergic receptor that is expressed on OPCs and promotes their survival as well as their proliferation (35); the *P2X4* gene was elevated in OPCs of Ad-PPAR-γ–treated kits with IVH relative to controls with IVH. The *ADCY10* gene (36), which encodes soluble adenyl cyclase enzyme catalyzing formation of cyclic AMP, was elevated in OPCs of Ad-PPAR-γ–treated kits with IVH relative to controls. Increased cyclic AMP promotes myelination (37). Two genes having roles in fatty acid degradation, including *ALDH9* (aldehyde dehydrogenase 9) and CPT1 (carnitine O-palmitoyl transferase 1), were diminished in Ad-PPAR-γ–treated kits with IVH relative to controls, which will result in accumulation of fat in the OPCs. Two genes for the glycolytic pathway—*GPI* (Glucose-6-phosphate isomerase) and *GAPDHS* (Glyceraldehyde-3-phosphate dehydrogenase) enzymes–were reduced in OPCs of Ad-PPAR-γ–treated kits. Furthermore, the down-regulation of the *ND3* gene would likely reduce oxidative phosphorylation, and the elevation of *PDK2* would promote lactate formation in Ad-PPAR-γ–treated kits with IVH.

Cell cycle genes, including *cyclin E2*, *CENPE*, *CENPF*, *CEP89*, *CLK1*, *CKAP2*, and *CKAP5*, were reduced in OPCs of Ad-PPAR-γ–treated animals, suggesting an underlying mechanism of PPAR-γ–induced reduced proliferation and consequent, enhanced maturation of OPCs. Antioxidants, including *GGT7* (glutathione hydrolase 7), *GPX7* (glutathione peroxidase), *GLOD4*, (glyoxalase 1) and HSPA5 (heat shock protein), were elevated in Ad-PPAR-γ–treated kits with IVH relative to controls, thereby offering protection to OPCs against IVH-induced free radicals. The extracellular matrix plays an important role in cell adhesion and migration of OPCs. An elevation in collagen type V alpha 3 chain (COL5A3) and reduction in angiopoietin 2, integrin subunit alpha 10 (*ITGA10*), and hyaluronan mediated motility receptor in PPAR-γ–treated kits (relative to controls) might contribute in promoting the migration of OPCs. A significant elevation in the PPAR-γ gene in OPCs by sevenfold indicates that the changes in OPC transcriptome are primarily PPAR-γ–induced (Fig. 8*A*). However, microglial changes would also contribute to these differences.

Olig1, Olig2, and Sox10 genes were comparable between the two groups, whereas the four key OPC genes regulating myelination, including *MBP*, *MAG*, myelin-associated oligodendrocyte basic protein, and myelin protein zero like 1, showed a strong trend toward elevation in Ad-PPAR-γ–treated kits with IVH (WIR values: 12.7, 1.8, 3.6, and 3.8, respectively; Fig. 8*C*). RNA-seq of OPCs discovers PPAR-γ–induced genes that would increase *P2X4* expression, cyclic AMP production, and fatty acid synthesis but slow down the cell cycle progression in OPCs, thereby contributing to OPC maturation and enhanced myelination.

Discussion

IVH remains a major complication of prematurity, which results in reduced myelination of the periventricular white matter and neurological deficits in the survivors (5, 7). No tangible therapeutic treatment is currently available for these infants. In the present study, we found that PPAR-γ activation reduced inflammation, promoted OPC maturation, and enhanced myelination in kits with IVH. In addition, PPAR-γ activation increased CD36 expression in microglia and promoted microglial phagocytosis but did not reduce hydrocephalus. Transcriptomic analyses of the isolated OPCs showed that PPAR-γ–induced up-regulation of the genes for purinergic signaling and cyclic adenosine monophosphate and that antioxidant production likely contributed to enhanced maturation of OPCs and myelination. In addition, RNA-seq of isolated microglia identified that PPAR-γ triggered

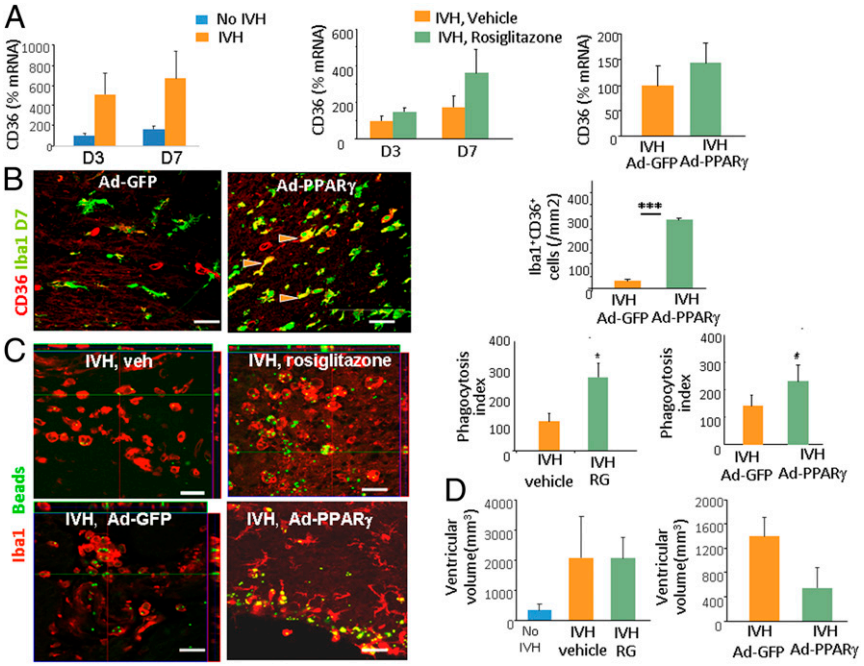

Fig. 6. PPAR-γ activation increases CD36$^+$ microglia and phagocytosis but does not reduce hydrocephalus. (*A*) The mRNA expression of CD36 was quantified by RT-qPCR using TaqMan probes. Bar charts are mean ± SEM ($n = 5$ in each group). IVH resulted in a trend toward elevation in the mRNA expression of CD36; however, the comparison was not significant. Rosiglitazone or Ad-PPAR-γ treatment did not affect CD36 expression. (*B*) Representative immunofluorescence is shown in cryosections of 7-d-old kits double-labeled with Iba1- and CD36-specific antibodies. The density of Iba1$^+$CD36$^+$ microglia (arrowhead) were higher in Ad- PPAR-γ–treated kits with IVH relative Ad-GFP controls with IVH. (Scale bar, 20 μm.) (*C*) Rabbit kits with IVH treated with rosiglitazone or Ad-PPAR-γ virus. The 2.5-μL fluorescent beads (green) were injected in ventricles at 24 h age, and kits were euthanized at 72 h. Coronal sections were stained with Iba1 antibody. *Upper* panel and *Left Lower* panel are orthogonal views in *x–z* and *y–z* planes of a composite z-stack of a series of confocal images taken 0.5 mm apart. Note abundance of the beads in the microglia of rosiglitazone- and Ad-PPAR-γ–treated kits. (Scale bar, 20 μm.) Bar charts are mean ± SEM ($n = 5$ in each group). The phagocytosis index was greater in rosiglitazone- and Ad-PPAR-γ–treated kits compared with controls. (*D*) Ventricle volume was measured by head ultrasound at D14. Ventricle volume was comparable between (*A*) rosiglitazone and vehicle controls as well as (*B*) Ad-PPAR-γ and Ad-GFP–treated kits. *$P < 0.05$, ***$P < 0.001$.

the down-regulation of several proinflammatory genes and transcripts having roles in Parkinson's disease and amyotrophic lateral sclerosis, which seemingly promoted neurological recovery in kits with IVH. The strengths of the present study are the use of human tissues to assess the effect of IVH on PPAR-γ expression, use of both pharmacological and genetic intervention to assess the effect of PPAR-γ activation on myelination, transcriptomic analyses highlighting the underlying mechanisms, and neurobehavioral profile. Together, these studies suggest a mechanism-based strategy to promote myelination and neurological recovery in newborns with IVH.

Our data have firmly established that PPAR-γ activation promotes OPC maturation and myelination in rabbit kits with IVH. We employed adenovirus delivery of the PPAR-γ gene to overexpress PPAR-γ and rosiglitazone for activating the PPAR-γ signaling cascade. Both the modes of therapy showed that PPAR-γ stimulation enhanced myelination in kits with IVH. We tested proliferation and maturation of OPCs in rosiglitazone-treated kits, which demonstrated that rosiglitazone promoted maturation of OPCs but not the proliferation of OPCs. Consistent with our experiments, previous studies have shown that PPAR-γ agonists, including pioglitazone and 14-deoxy prostaglandin J2, protect oligodendrocytes and promote their maturation in culture experiments (18). In addition, rosiglitazone treatment significantly ameliorates white matter injury and increases both OPC proliferation and maturation in an adult mouse model of middle cerebral artery occlusion (38). Furthermore, PPAR-γ agonists confer neuroprotection in animal models of a wide range of neurological disorders involving white matter, including demyelinating and neurodegenerative diseases, traumatic injuries, and stroke (20, 21), which reinforces our findings that use of PPAR-γ agonists or PPAR-γ overexpression enhances OPC maturation and myelination in kits with IVH.

PPAR-γ activation by rosiglitazone up-regulates CD36 expression, differentiates microglia into protective phenotype, promotes hematoma absorption, and protects brain cells in an adult model of intracranial hemorrhage (ICH) (11, 39). Accordingly, we found that PPAR-γ activation increased microglial phagocytic activity and CD36 expression in kits with IVH. However, this failed to minimize hydrocephalus in kits with IVH. A previous study has shown that inhibiting inflammation by targeting TLR4-NFkB signaling reduces CSF production and hydrocephalus (40). However, in the present study, PPAR-γ–induced suppression of inflammation and increased microglial phagocytosis did not affect the ventricle size. This might be because of multifactorial pathogenesis of post-IVH hydrocephalus, which is attributed to reduced CSF absorption, obstructed CSF circulation, and increased CSF production (41).

Several studies have reported that PPAR-γ is expressed primarily on neurons and astrocytes of adult humans and mice (12, 42). In addition, PPAR-γ expression has been confirmed in purified rat oligodendrocyte cultures (14). In contrast, we found that PPAR-γ expression was weak to absent on astrocytes, microglia, and OPCs in the frontoparietal telencephalon of premature human infants and rabbit kits without IVH. However, the occurrence of IVH robustly induced PPAR-γ expression on microglia but weakly on OPCs and astrocytes. This discrepancy in the expression of PPAR-γ on glial cells between present and previous studies can be attributed to the inclusion of developing brains in our study as opposed to adult brains in the previous reports. Ad-PPAR-γ

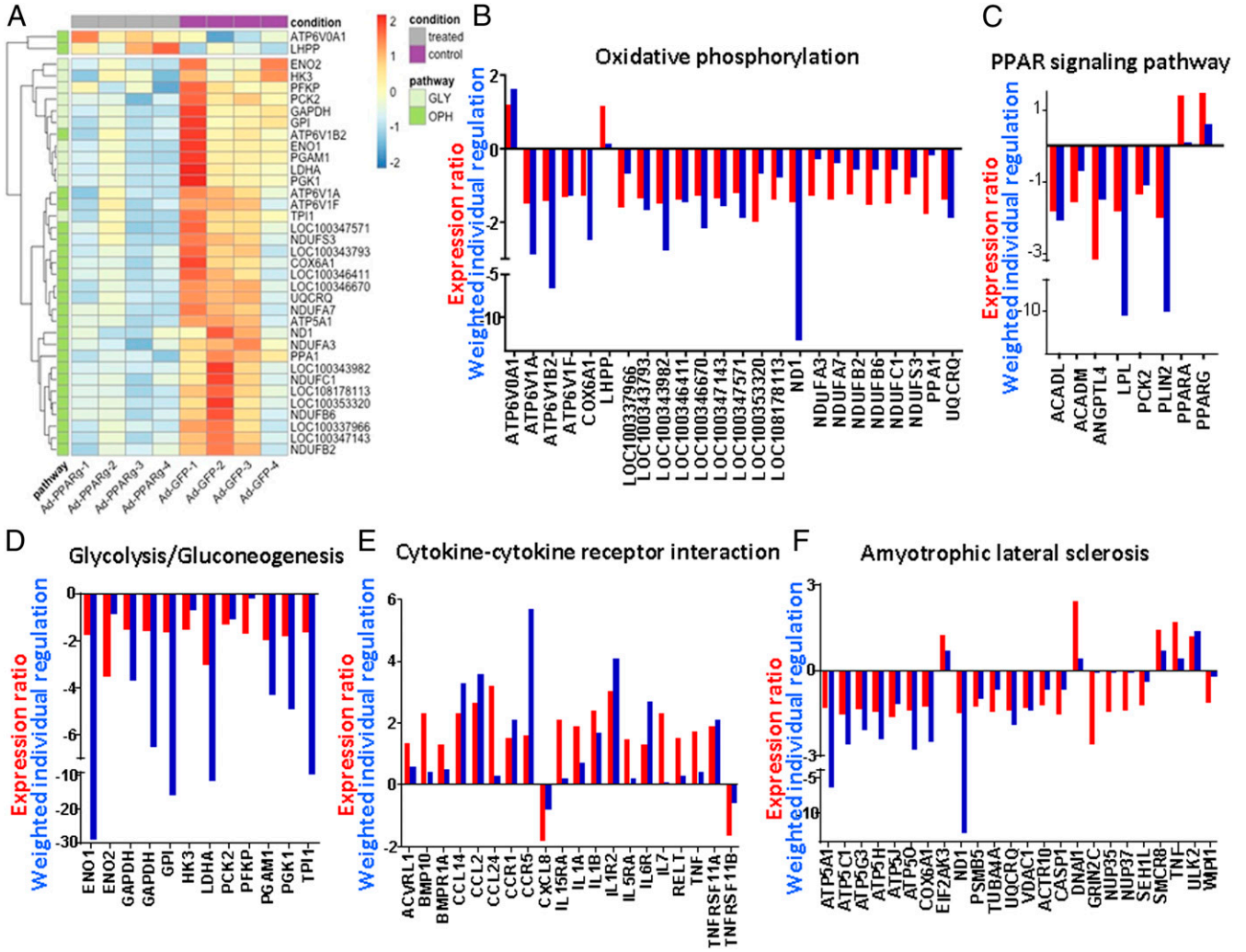

Fig. 7. Transcriptional profile of microglia in Ad-PPAR-γ–treated kits compared with Ad-GFP controls: $CD45^{Low}/CD11b^{+}$ microglia were sorted by FACS from the cerebral hemisphere of Ad-PPAR-γ and Ad-GFP treated rabbit kits with IVH at D7. Total RNA was extracted, and RNA-seq was performed. (*A*) Heat map shows relative expression of genes for oxidative phosphorylation (OPH) and glycolytic (GLY) pathways across brain samples ($n = 4$ each). (*B*) Bar chart shows gene expression ratio (*x*, red bar, negative for down-regulation and positive for down-regulation) and WIR (blue bar, negative for down-regulation and positive for down-regulation) for the genes of OPH. Note, Ad-PPARγ induces significant down-regulation of genes for OPH. (*C*) Bar graph shows significant changes in the gene expression ratio and WIR for the molecules of PPAR-γ signaling pathway. (*D*) Bar chart shows gene expression ratio and WIR. Note, Ad-PPAR-γ induces significant down-regulation of genes for the glycolytic pathway. (*E*) Bar chart depicts the gene expression ratio and WIR. Note, Ad-PPAR-γ induces significant alteration of genes for cytokine–cytokine receptor interaction (inflammation). (*F*) Bar graph shows the gene expression ratio and WIR. Note, Ad-PPAR-γ induces significant alteration of genes for amyotrophic lateral sclerosis.

treatment led to a significant elevation in PPAR-γ mRNA expression both in the microglia (x = 1.48x, Fig. 7*C*) and OPCs (x = 7.45x, Fig. 8*A*). Moreover, about 18% of $O4^{+}$ OPCs expressed PPAR-γ in the periventricular region in Ad-PPAR-γ–treated kits compared with less than 1% in Ad-GFP–treated kits (*SI Appendix*, Fig. S2). Hence, the effect on oligodendrocyte transcriptome, maturation, and myelin formation is likely to be directly induced by Ad-PPAR-γ treatment. However, microglia-induced attenuation in inflammation would also contribute to the improvement in myelination (19).

There is a wealth of literature suggesting that PPAR-γ agonists have major therapeutic potential in a wide spectrum of brain disorders. It regulates anti-inflammatory mechanisms, reduces oxidative stress, and promotes neurogenesis, neuronal differentiation, and angiogenesis (14, 42). It confers neuroprotection in cerebral ischemic, traumatic, demyelinating, and degenerative brain diseases. Rosiglitazone and pioglitazone reduce infarct volume in a murine model of cerebral ischemia and minimize neurological deficit in an adult model of intracranial hemorrhage (10, 11, 21, 39). These PPAR-γ agonists reduce neuronal damage, microglia activation, and myelin loss in spinal cord injury and alleviate clinical symptoms in experimental autoimmune encephalomyelitis (43, 44). They down-regulate proinflammatory genes and ameliorate mitochondrial function (45). All these studies reinforce our findings that rosiglitazone or Ad-PPAR-γ treatment enhances myelination and neurological recovery in premature rabbits with IVH. Hence, rosiglitazone has the potential to be considered for a clinical trial in premature infants with IVH, as the worrisome side effect of cardiac ischemia is not relevant to newborns.

To understand the mechanisms of PPAR-γ–induced restoration in OPC maturation and myelination in kits with IVH, we performed RNA-seq analysis of $O4^{+}$ OPCs and $CD45^{Low}/CD11b^{+}$ microglia isolated from the cerebral hemispheres of preterm kits with IVH, who were treated with either Ad-PPAR-γ or Ad-GFP. Transcriptomic analyses of OPCs revealed that the expression of *P2X4* and *ADCY10* genes were elevated in OPCs of Ad-PPAR-γ–treated

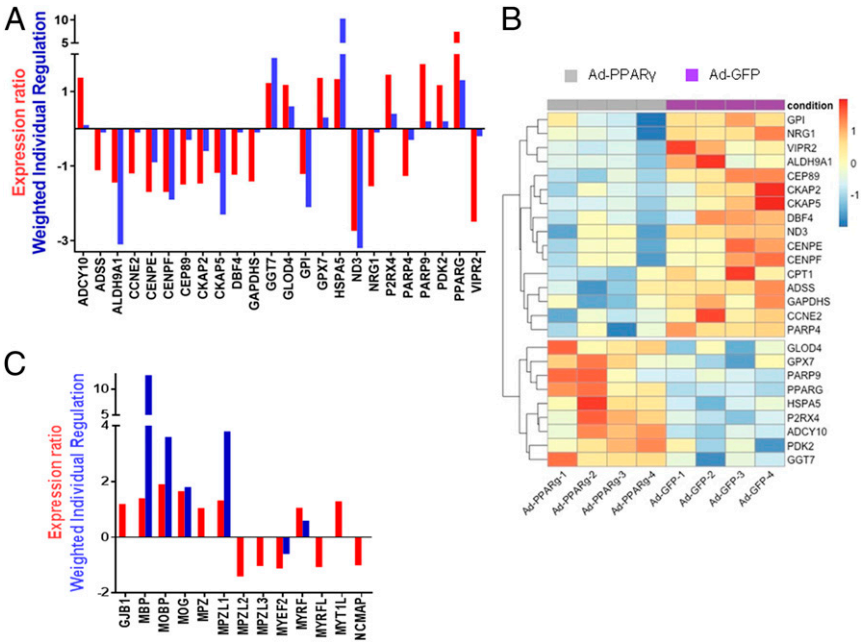

Fig. 8. Transcriptional profile of OPC in Ad-PPAR-γ–treated kits compared with Ad-GFP kits: (*A*) O4$^+$ OPCs were sorted by FACS from the cerebral hemisphere of Ad-PPAR-γ– and Ad-GFP–treated rabbit kits with IVH at D7. Total RNA was extracted, and RNA-seq was performed. Bar chart shows the gene expression ratio (*x*, red bar) and (*B*) WIR (blue bar) of Ad-PPAR-γ–treated versus Ad-GFP kits. Note, Ad-PPAR-γ induced significant up- or down-regulation of genes in OPCs. (*B*) Heat map shows relative expression of genes for OPCs across brain samples ($n = 4$ each). (*C*) Bar chart shows some important genes having role in myelination, which are substantially different between groups. However, the comparison did not reach statistical significance owing to large biological variability.

kits compared with controls. P2X4 is a purinergic receptor expressed on OPCs and microglia, which is activated by ATP (46). In vitro studies have shown that ATP or its derivative, released by unmyelinated axons, can affect OPC proliferation, maturation, and myelination (35). The P2X4 receptor also controls microglia activation and favors remyelination in autoimmune encephalitis (47). The *ADCY10* gene forms the soluble adenyl cyclase enzyme catalyzing formation of cyclic AMP (36). Increased cyclic AMP promotes differentiation of OPCs and myelination (37). These findings strengthen the concept that up-regulation of the *P2X4* and *ADCY10* genes of the purinergic signaling pathway can promote myelination in Ad-PPAR-γ–treated kits with IVH. Moreover, escalated transcription of the glutathione peroxidase (GPX7) and Glyoxalase domain 4 (*GLOD4*) genes would confer protection to OPCs. GPX7 detoxifies H_2O_2 and is an antioxidant enzyme in humans. Glyoxalase disposes of endogenous toxins, recycles reactive metabolites, and forms glutathione and is thus neuroprotective. PPAR-γ–triggered down-regulation of cell cycle genes—*cyclin E2*, *CENPE*, *CENPF*, and others—would slow down cell cycle progression and enhance maturation of OPCs. These transcriptomic changes in OPCs appear to be directly induced by Ad-PPAR-γ and also partly related to diminution in inflammation. Together, the integration of the PPAR-γ gene reprograms OPC function by increasing the transcription of several genes that can ameliorate myelination of the white matter.

Previous studies have demonstrated that PPAR-γ activation reduces inflammation and oxidative stress in an adult model of intracranial hemorrhage by diminishing the expression of proinflammatory cytokines, matrix MMP9, inducible nitric oxide synthase, and extracellular H_2O_2 level (11). Consistent with these findings, transcriptomic analyses of isolated microglia in Ad-PPAR-γ–treated kits showed down-regulation of MMP-9 and several proinflammatory genes. This is an important demonstration of PPAR-γ–induced down-regulation of gene for *MIF*, kynurenine 3-monooxygenase (*KMO*), annexin-A1, -A2, -A3, -A4, -A5, and S100A9 in cerebral inflammation induced by ventricular/cerebral hemorrhage, which would inhibit inflammation. While PPAR-γ gene delivery favorably elevated interleukin1-receptor 2 (suppressor of IL-1) and interferon regulatory factor 7, it also increased transcripts of several cytokines and chemokines that can potentially worsen IVH-induced cerebral inflammation. PPAR-γ agonists reduce cerebral inflammation in Parkinson's disease, amyotrophic lateral sclerosis, and Alzheimer's disease (8, 20). Intriguingly, our analyses also showed that genes for these three neurological diseases were down-regulated in the microglia of Ad-PPAR-γ–treated animals (Fig. 7 and *SI Appendix*, Fig. S5). Since microglia development undergoes three stages of maturation in mice, including early microglia (until E14), premicroglia (E14-P45), and adult microglia (after P45), our analyses of premicroglia are not comparable with experiments performed on adult microglia in adult rodent models (11). Indeed, premicroglia and adult microglia exhibit vast differences in the genetic and epigenetic profile as well as their reactivity to injury (48).

In conclusion, the present study highlights the neuroprotective effect of PPAR-γ activation in promoting myelination and enhancing the neurological recovery of premature rabbit kits with IVH. However, this strategy does not reduce hydrocephalus despite activation of the CD36 phagocytic receptors and increase in microglial phagocytic response in rabbit kits with IVH. Moreover, the study uncovers the identity of previously unrecognized PPAR-γ–induced genes that reprogramed microglia and OPC, leading to improved myelination and clinical recovery in newborns with IVH. PPAR-γ is an important target that has an immense therapeutic potential, which is yet to be exploited in preterm infants.

Materials and Methods

Animals. This study was approved by the Institutional Animal Care and Use Committee of Albert Einstein College of Medicine, Bronx, NY. We used our preterm rabbit model of glycerol-induced IVH that has been extensively validated in our previous studies (3, 4, 19, 25, 26, 49). Timed-pregnant New Zealand rabbits were purchased from Charles River Laboratories, Inc. We performed Caesarean sections to deliver the preterm kits at 29 d of gestational

age (full-term = 32 d). Newborn kits were reared in an infant incubator at a temperature of 35 °C. To produce IVH, we treated rabbit kits of either sex with 50% glycerol (6.5 gm/kg) intraperitoneally at 3 to 4 h age. IP glycerol induces IVH by causing intravascular dehydration and an increase in serum osmolality, which reduces intracranial pressure and ruptures fragile vessels in the ganglionic eminence (3, 50). We used rabbit milk replacer (Wombaroo, Glen Osmond) to gavage-feed the kits in a volume of 2 to 4 mL every 12 h (100 mL/kg/day) for the first 2 d, and then feeds were advanced to 125, 150, 200, 250, and 280 mL/kg at postnatal days 3, 5, 7, 10, and 14, respectively. The severity of IVH was assessed by measuring ventricular volume (length × breadth × depth in coronal and sagittal views) on head ultrasound at 24 h age by employing an ultrasound machine (Acuson ×700, Siemens). Kits with IVH were graded as moderate (70 to 150 mm^3) and severe (151 to 250 mm^3) IVH on the basis of ventricular volumes (Fig. 3*A*). A ventricular volume of less than 70 mm^3 suggested an absence of IVH or presence of microscopic bleed(s). We randomized the rabbit kits with moderate and severe into treatment or control groups in such a fashion that the severity of IVH was comparable between the groups.

Rosiglitazone or Ad-PPAR-γ Treatment, Human and Rabbit Tissue Collection and Processing, Immunohistochemistry, Stereological Quantification of Cells, RT-qPCR, and Western Blot Analysis. Described in *SI Appendix, Supplemental Methods*.

Electron Microscopy and Flow Cytometry. Described in *SI Appendix, Supplemental Methods*.

RNA-seq. RNA extraction, library preparations, sequencing reactions, and bioinformatic analysis were carried out by GENEWIZ, LLC. RNA samples were extracted using TRIzol (Invitrogen). Extracted samples were quantified by Qubit 2.0 Fluorometer (Life Technologies), and RNA integrity was measured using the RNA Screen Tape on Agilent 2200 TapeStation (Agilent Technologies). RNA-seq libraries were prepared and validated using DNA Analysis Screen Tape on the Agilent 2200 TapeStation (Agilent Technologies) and quantified using Qubit 2.0 Fluorometer (Invitrogen) as well as by qPCR (KAPA Biosystems). The pooled libraries were clustered on a flowcell, which was loaded on the Illumina HiSeq instrument (4000) according to manufacturer's instructions and sequenced using a 2 × 150 bp Paired End configuration. Image analysis and base calling were conducted by the HiSeq Control Software. Raw sequence data (.bcl files) generated from Illumina HiSeq were converted into fastq files and demultiplexed using Illumina's bcl2fastq 2.17 software. One mismatch was allowed for index sequence identification.

The trimmed reads were mapped to the *Rabbit Oryctolagus* reference genome available on ENSEMBL using the STAR aligner version 2.5.2b. The STAR aligner is a splice aligner that detects splice junctions and incorporates them to help align the entire read sequences. BAM files were generated as a result of this step. Unique gene hit counts were calculated by using feature Counts from the Subread package version 1.5.2. Only unique reads that fell within exon regions were counted. Using DESeq2, a comparison of gene expression between the groups of samples was performed. Genes with less than 10 raw counts in any sample were removed from the analysis. Expression data were processed according to our standard procedure (51). Thus, the adequately quantified genes were normalized to the median, and the average expression level (*AVE*) and coefficient of variation among biological replicas (*CV*) were computed for every gene in each group of samples. A gene was considered as significantly differentially expressed between two groups of samples *A* and *B* if the absolute expression ratio (*x*, negative for down-regulation) exceeded the fold-change cutoff computed for that gene (*CUT*). *CUT* takes into account the combined effect of the technical noise and the biological variability among the considered biological replicas:

$$\left|x_i^{(A/B)}\right| > CUT_i^{(A/B)} = 1 + \sqrt{2\left(\left(CV_i^{(A)}\right)^2 + \left(CV_i^{(B)}\right)^2\right)}, \text{ where } x_i^{A/B} = \begin{cases} \dfrac{AVE_i^{(A)}}{AVE_i^{(B)}} & \text{if} \quad AVE_i^{(A)} \geq AVE_i^{(B)} \\ -\dfrac{AVE_i^{(B)}}{AVE_i^{(A)}} & \text{if} \quad AVE_i^{(B)} \geq AVE_i^{(A)} \end{cases}.$$

Traditional percentages of up-/down-regulated genes consider the genes as uniform +1/−1 contributors to the transcriptomic alteration. However, in this report, in addition to the expression ratios, transcriptomic differences among groups of samples were also presented as WIR:

$$WIR_i^{(A/B)} = \underbrace{\frac{x_i^{(A/B)}}{\left|x_i^{(A/B)}\right|}}_{\text{reference}} \underbrace{AVE_i^{(B)}}_{\text{expression}} \underbrace{\left(\left|x_i^{(A/B)}\right| - 1\right)}_{\text{net regulation}} \underbrace{\left(1 - p_i^{(A/B)}\right)}_{\text{confidence}}, \text{ where}$$

$$p_i^{(A/B)} = p - value\ of\ the\ heteroscedastic\ t - test\ of\ means'\ equality.$$

WIR is not limited to the significantly regulated genes based on an arbitrarily introduced criterion but considers the contributions of all genes. Moreover, the net regulation is weighted by the expression level in the reference sample and modulated by the statistical confidence in the expression difference. Average WIR of the genes included in a particular pathway gives the weighted pathway regulation of that pathway. Genes involved in selected pathways were selected from KEGG (https://www.genome.jp/kegg/pathway.html) using our Pathway software (52).

Statistics and Analysis. The data are presented as means ± SEM. To compare the levels of MBP, MAG and cytokines, mRNA, protein, and counts between two groups (IVH versus no IVH, Ad-PPARγ versus Ad-GFP, or vehicle versus rosiglitazone), we used a *t* test. To assess the difference between the three groups no glycerol, glycerol no IVH and IVH, a one-way ANOVA was used. To compare the mRNA expression between kits with and without IVH at D3 and D7 age, we employed a two-way ANOVA. All post hoc comparisons between means were done by Tukey's multiple comparison test at 0.05.

Data Availability. Sequencing data were deposited in the National Center for Biotechnology Information Gene Expression Omnibus (accession no. GSE182520). All other study data are included in the article and/or supporting information.

ACKNOWLEDGMENTS. This study is supported by funding from NIH Grant R21NS102897 (P.B.) and Grant RO1 NS110760 (P.B.).

1. P. Ballabh, Intraventricular hemorrhage in premature infants: Mechanism of disease. *Pediatr. Res.* **67**, 1–8 (2010).
2. J. D. Horbar *et al.*; Members of the Vermont Oxford Network, Trends in mortality and morbidity for very low birth weight infants, 1991-1999. *Pediatrics* **110**, 143–151 (2002).
3. P. Georgiadis *et al.*, Characterization of acute brain injuries and neurobehavioral profiles in a rabbit model of germinal matrix hemorrhage. *Stroke* **39**, 3378–3388 (2008).
4. C. O. Chua *et al.*, Consequences of intraventricular hemorrhage in a rabbit pup model. *Stroke* **40**, 3369–3377 (2009).
5. D. L. Armstrong, C. D. Sauls, J. Goddard-Finegold, Neuropathologic findings in short-term survivors of intraventricular hemorrhage. *Am. J. Dis. Child.* **141**, 617–621 (1987).
6. D. I. Rushton, P. R. Preston, G. M. Durbin, Structure and evolution of echo dense lesions in the neonatal brain. A combined ultrasound and necropsy study. *Arch. Dis. Child.* **60**, 798–808 (1985).
7. S. Bolisetty *et al.*; New South Wales and Australian Capital Territory Neonatal Intensive Care Units' Data Collection, Intraventricular hemorrhage and neurodevelopmental outcomes in extreme preterm infants. *Pediatrics* **133**, 55–62 (2014).
8. N. Nicolakakis, E. Hamel, The nuclear receptor PPARgamma as a therapeutic target for cerebrovascular and brain dysfunction in Alzheimer's disease. *Front. Aging Neurosci.* **2**, 21 (2010).
9. R. Kapadia, J. H. Yi, R. Vemuganti, Mechanisms of anti-inflammatory and neuroprotective actions of PPAR-gamma agonists. *Front. Biosci.* **13**, 1813–1826 (2008).
10. T. Shimazu *et al.*, A peroxisome proliferator-activated receptor-gamma agonist reduces infarct size in transient but not in permanent ischemia. *Stroke* **36**, 353–359 (2005).
11. X. Zhao *et al.*, Hematoma resolution as a target for intracerebral hemorrhage treatment: Role for peroxisome proliferator-activated receptor gamma in microglia/macrophages. *Ann. Neurol.* **61**, 352–362 (2007).
12. M. O. Fernandez *et al.*, Astrocyte-specific deletion of peroxisome-proliferator activated receptor-γ impairs glucose metabolism and estrous cycling in female mice. *J. Endocr. Soc.* **1**, 1332–1350 (2017).
13. A. Warden *et al.*, Localization of PPAR isotypes in the adult mouse and human brain. *Sci. Rep.* **6**, 27618 (2016).
14. A. Bernardo, L. Minghetti, Regulation of glial cell functions by PPAR-gamma natural and synthetic agonists. *PPAR Res.* **2008**, 864140 (2008).
15. U. Beisiegel, A. A. Spector, Lipids and lipoproteins in the brain. *Curr. Opin. Lipidol.* **12**, 243–244 (2001).
16. L. Fajas, M. B. Debril, J. Auwerx, PPAR gamma: An essential role in metabolic control. *Nutr. Metab. Cardiovasc. Dis.* **11**, 64–69 (2001).
17. R. Walczak, P. Tontonoz, PPARadigms and PPARadoxes: Expanding roles for PPAR-gamma in the control of lipid metabolism. *J. Lipid Res.* **43**, 177–186 (2002).

18. A. Bernardo, D. Bianchi, V. Magnaghi, L. Minghetti, Peroxisome proliferator-activated receptor-gamma agonists promote differentiation and antioxidant defenses of oligodendrocyte progenitor cells. *J. Neuropathol. Exp. Neurol.* **68**, 797–808 (2009).
19. G. Vinukonda *et al*., Neuroprotection in a rabbit model of intraventricular haemorrhage by cyclooxygenase-2, prostanoid receptor-1 or tumour necrosis factor-alpha inhibition. *Brain* **133**, 2264–2280 (2010).
20. T. Breidert *et al*., Protective action of the peroxisome proliferator-activated receptor-gamma agonist pioglitazone in a mouse model of Parkinson's disease. *J. Neurochem.* **82**, 615–624 (2002).
21. B. Schütz *et al*., The oral antidiabetic pioglitazone protects from neurodegeneration and amyotrophic lateral sclerosis-like symptoms in superoxide dismutase-G93A transgenic mice. *J. Neurosci.* **25**, 7805–7812 (2005).
22. Xia P *et al*., Pioglitazone confers neuroprotection against ischemia-induced pyroptosis due to its inhibitory effects on HMGB-1/RAGE and Rac1/ROS pathway by activating PPAR. *Cell. Physiol. Biochem.* **45**, 2351–2368 (2018).
23. P. D. Storer, J. Xu, J. Chavis, P. D. Drew, Peroxisome proliferator-activated receptor-gamma agonists inhibit the activation of microglia and astrocytes: Implications for multiple sclerosis. *J. Neuroimmunol.* **161**, 113–122 (2005).
24. P. D. Drew, J. Xu, M. K. Racke, PPAR-gamma: Therapeutic potential for multiple sclerosis. *PPAR Res.* **2008**, 627463 (2008).
25. L. R. Vose *et al*., Treatment with thyroxine restores myelination and clinical recovery after intraventricular hemorrhage. *J. Neurosci.* **33**, 17232–17246 (2013).
26. K. Dummula *et al*., Bone morphogenetic protein inhibition promotes neurological recovery after intraventricular hemorrhage. *J. Neurosci.* **31**, 12068–12082 (2011).
27. J. Bloom, S. Sun, Y. Al-Abed, MIF, a controversial cytokine: A review of structural features, challenges, and opportunities for drug development. *Expert Opin. Ther. Targets* **20**, 1463–1475 (2016).
28. S. Ning, J. S. Pagano, G. N. Barber, IRF7: Activation, regulation, modification and function. *Genes Immun.* **12**, 399–414 (2011).
29. F. F. Vasilyev, A. N. Silkov, S. V. Sennikov, Relationship between interleukin-1 type 1 and 2 receptor gene polymorphisms and the expression level of membrane-bound receptors. *Cell. Mol. Immunol.* **12**, 222–230 (2015).
30. H. R. Kim *et al*., An essential role for TAGLN2 in phagocytosis of lipopolysaccharide-activated macrophages. *Sci. Rep.* **7**, 8731 (2017).
31. T. O'Connor, L. Borsig, M. Heikenwalder, CCL2-CCR2 signaling in disease pathogenesis. *Endocr. Metab. Immune Disord. Drug Targets* **15**, 105–118 (2015).
32. D. W. Raible, F. A. McMorris, Oligodendrocyte differentiation and progenitor cell proliferation are independently regulated by cyclic AMP. *J. Neurosci. Res.* **34**, 287–294 (1993).
33. V. E. Morrison, V. N. Smith, J. K. Huang, Retinoic acid is required for oligodendrocyte precursor cell production and differentiation in the postnatal mouse corpus callosum. *eNeuro* **7**, ENEURO.0270-19.2019 (2020).
34. D. Marangon, M. Boccazzi, D. Lecca, M. Fumagalli, Regulation of oligodendrocyte functions: Targeting lipid metabolism and extracellular matrix for myelin repair. *J. Clin. Med.* **9**, E470 (2020).
35. T. Ozaki *et al*., The P2X4 receptor is required for neuroprotection via ischemic preconditioning. *Sci. Rep.* **6**, 25893 (2016).
36. S. Pozdniakova, Y. Ladilov, Functional significance of the Adcy10-dependent intracellular cAMP compartments. *J. Cardiovasc. Dev. Dis.* **5**, E29 (2018).
37. F. S. Afshari, A. K. Chu, C. Sato-Bigbee, Effect of cyclic AMP on the expression of myelin basic protein species and myelin proteolipid protein in committed oligodendrocytes: Differential involvement of the transcription factor CREB. *J. Neurosci. Res.* **66**, 37–45 (2001).
38. L. Han *et al*., Rosiglitazone promotes white matter integrity and long-term functional recovery after focal cerebral ischemia. *Stroke* **46**, 2628–2636 (2015).
39. X. Zhao, Y. Zhang, R. Strong, J. C. Grotta, J. Aronowski, 15d-Prostaglandin J2 activates peroxisome proliferator-activated receptor-gamma, promotes expression of catalase, and reduces inflammation, behavioral dysfunction, and neuronal loss after intracerebral hemorrhage in rats. *J. Cereb. Blood Flow Metab.* **26**, 811–820 (2006).
40. J. K. Karimy *et al*., Inflammation-dependent cerebrospinal fluid hypersecretion by the choroid plexus epithelium in posthemorrhagic hydrocephalus. *Nat. Med.* **23**, 997–1003 (2017).
41. J. E. Koschnitzky *et al*., Opportunities in posthemorrhagic hydrocephalus research: Outcomes of the Hydrocephalus Association Posthemorrhagic Hydrocephalus Workshop. *Fluids Barriers CNS* **15**, 11 (2018).
42. S. Villapol, Roles of peroxisome proliferator-activated receptor gamma on brain and peripheral inflammation. *Cell. Mol. Neurobiol.* **38**, 121–132 (2018).
43. A. Diab *et al*., Peroxisome proliferator-activated receptor-gamma agonist 15-deoxy-Delta(12,14)-prostaglandin J(2) ameliorates experimental autoimmune encephalomyelitis. *J. Immunol.* **168**, 2508–2515 (2002).
44. S. W. Park *et al*., Thiazolidinedione class of peroxisome proliferator-activated receptor gamma agonists prevents neuronal damage, motor dysfunction, myelin loss, neuropathic pain, and inflammation after spinal cord injury in adult rats. *J. Pharmacol. Exp. Ther.* **320**, 1002–1012 (2007).
45. D. L. Feinstein *et al*., Receptor-independent actions of PPAR thiazolidinedione agonists: Is mitochondrial function the key? *Biochem. Pharmacol.* **70**, 177–188 (2005).
46. T. G. Welsh, S. Kucenas, Purinergic signaling in oligodendrocyte development and function. *J. Neurochem.* **145**, 6–18 (2018).
47. A. Zabala *et al*., P2X4 receptor controls microglia activation and favors remyelination in autoimmune encephalitis. *EMBO Mol. Med.* **10**, e8743 (2018).
48. O. Matcovitch-Natan *et al*., Microglia development follows a stepwise program to regulate brain homeostasis. *Science* **353**, aad8670 (2016).
49. P. Dohare *et al*., Glycogen synthase kinase-3β inhibition enhances myelination in preterm newborns with intraventricular hemorrhage, but not recombinant Wnt3A. *Neurobiol. Dis.* **118**, 22–39 (2018).
50. P. Ballabh *et al*., Angiogenic inhibition reduces germinal matrix hemorrhage. *Nat. Med.* **13**, 477–485 (2007).
51. D. A. Iacobas, Biomarkers, master regulators and genomic fabric remodeling in a case of papillary thyroid carcinoma. *Genes (Basel)* **11**, E1030 (2020).
52. S. Iacobas, N. Ede, D. A. Iacobas, The gene master regulators (GMR) approach provides legitimate targets for personalized, time-sensitive cancer gene therapy. *Genes (Basel)* **10**, E560 (2019).